# Temporal structure of chromatic channels revealed through masking

John Cass; Colin W. G. Clifford; David Alais; Branka Spehar

□ Author Affiliations

Journal of Vision May 2009, Vol.9, 17. doi: <a href="https://doi.org/10.1167/9.5.17">https://doi.org/10.1167/9.5.17</a>

## **Abstract**

The human color and luminance-driven systems appear to be mediated by mechanisms with distinct spatio-temporal tuning properties, with the iso-luminant color-driven system comparatively less sensitive to high rates of temporal modulation. While color and luminance defined speed and rate discrimination studies indicate perceptual access to the outputs of multiple, overlapping temporal frequency-selective mechanisms (channels), a detailed functional characterization of their response is currently restricted to the luminance-driven domain. Threshold elevations for 1- and 10-Hz targets were measured as a function of the temporal frequency of a spatio-temporally overlaid masking stimulus (1-30 Hz). Target and masking stimuli were iso-oriented gratings spatio-temporally modulated along each axis of human color space: L - M (red-green), S + S- (violet-yellow; S-cone isolating), and L + M + S (achromatic). Qualitatively equivalent patterns of temporal frequency-dependent masking were observed when measured within and, with one exception (red-green target, achromatic mask), between cardinal axes of human color space: fitted by one low-pass and one bandpass Gaussian function. That both low-pass and higher bandpass masking functions were evident between isoluminant cardinal color axes (L – M and S + S–) suggests that both low and high temporal frequency masking may be cortically mediated.

## Introduction

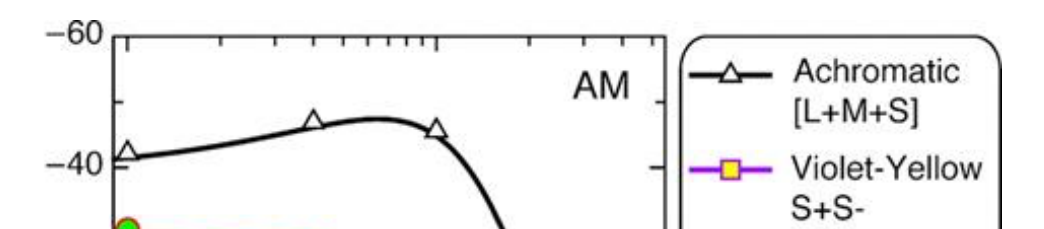
This site in the three classes of cone photoreceptor, characterized as predominantly long

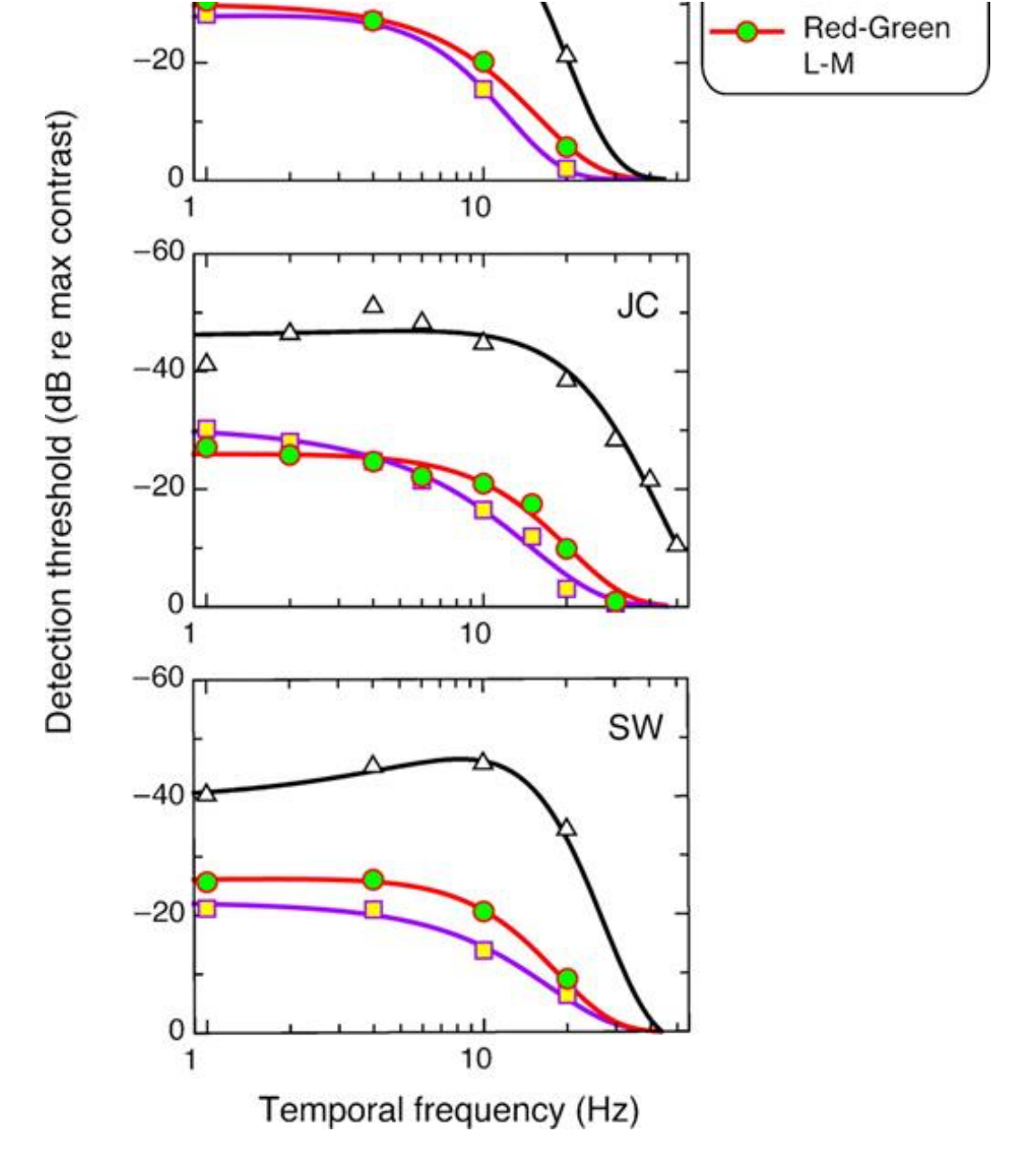
(L), medium (M), and short (S) wavelength selective (560, 530, and 420 nm, respectively; Brown & Wald, 1963, 1964; Dartnall, Bowmaker, & Mollon, 1983; MacLeod & Boynton, 1979; Rushton,

1962; Schnapf, Kraft, & Baylor, 1987; Sun, Smithson, Zaidi, & Lee, 2006). Following transduction, retinal ganglion cells integrate their cone afferents according to a strict pattern of chromatic combination generating a color space composed of three independent cardinal chromatic axes: S + S- (violet-yellow); L - M (red-green); and [L + M] (luminance) (Derrington, Krauskopf, & Lennie, 1984; MacLeod & Boynton, 1979) known as MBDKL space. While the responses of early parvocellular neurons demonstrate combinatorial integration of both red-green and luminance-selective afferents (De Monasterio & Gouras, 1975; Johnson, Hawken, & Shapley, 2004; Norren & Padmos, 1974), anatomical segregation of L - M and S + S- axes appears to be preserved in the responses of iso-luminant responsive neurons until primary visual cortex (V1), at which point neurons shift their chromatic preferences to include non-orthogonal regions of MBDKL space (Cottaris & De Valois, 1998; Derrington et al., 1984; Lennie, Krauskopf, & Sclar, 1990).

Several sources of human psychophysical evidence indicate that the iso-luminant chromatically driven visual system exhibits different temporal tuning characteristics to the luminance-driven system. For example, iso-luminant objects, across a broad range of spatio-temporal conditions, appear to move more slowly than luminance-defined objects (Cavanagh, Tyler, & Favreau, 1984; Mullen & Boulton, 1992; Ramachandran & Gregory, 1978) suggesting a chromatically driven response bias favoring lower temporal frequencies than the luminance-driven system. This interpretation is echoed in several detection paradigms. Not only are humans capable of detecting higher temporal rates of luminance modulation (30-50 Hz) compared with isoluminant modulation (~15 Hz; values known as the critical flicker fusion limits; de Lange, 1958; Shady, MacLeod, & Fisher, 2004) but chromatic contrast sensitivity (1/threshold) measured as a function of stimulus temporal frequency (known as the Modulation Transfer Function (MTF)) is comparatively more low pass than the luminance-driven MTF, which is more bandpass in shape, peaking between 4 and 10 Hz (see Figure 1) (Burr & Morrone, 1993, 1996; Eskew, Stromeyer, & Kronauer, 1994; Swanson, Ueno, Smith, & Pokorny, 1987; Uchikawa & Ikeda, 1986). Similar estimates have also been inferred when applying Fourier analysis to iso-luminant and luminance-defined Impulse Response Functions (IRFs) as measured by changes in sensitivity as a function of the inter-stimulus interval between successive stimulus pulses (Burr & Morrone, <u>1993</u>, <u>1996</u>; Eskew et al., <u>1994</u>; Swanson et al., <u>1987</u>; Uchikawa & Ikeda, <u>1986</u>).

## Figure 1





#### View Original Download Slide

Modulation transfer functions (MTFs) for vertical, spatio-temporally sinusoidally modulated gratings (1 c.p.d.) measured for three observers as a function of the temporal frequency of modulation within each cardinal color dimensions of MBDKL space. Data are each fitted with a single Gaussian function.

It has long been suggested that the luminance MTF may reflect the combined peak sensitivity

profiles of multiple temporal frequency-selective mechanisms (temporal channels; Hess & Snowden, 1992; Kelly, 1983; Metha & Mullen, 1996; Robson, 1966), a concept that is strongly analogous to the standard model relating spatial frequency channels to the contrast response function (Blakemore & Campbell, 1969a, 1969b). Evidence for multiple luminance-driven temporal channels has been found using several different psychophysical paradigms including

masking, temporal frequency discrimination and adaptation (Anderson & Duff, <u>1909</u>, fress & Snowden, <u>1992</u>; Langley & Bex, <u>2007</u>; Waugh & Hess, <u>1994</u>). While early studies proposed that both the perceived slowing and comparatively low-pass structure of the chromatic MTF implied that the chromatically driven system is likely to be mediated by a single low-pass temporal channel (Burr & Morrone, 1993, 1996; Eskew et al., 1994; Swanson et al., 1987; Uchikawa & Ikeda, 1986), more recent results indicate the existence of multiple temporal channels (Cropper, 1994; Metha & Mullen, 1996). Metha and Mullen (1996) tested the predictions of this single lowpass temporal channel model by having subjects undertake a chromatically defined [L – M] temporal frequency discrimination task at detection threshold, thereby obviating any cues relating to perceived contrast. This procedure yielded U-shaped discrimination threshold functions when expressed as a function of the standard's temporal frequency. That intermediate temporal frequencies were easier to discriminate than either low or high frequencies implies a greater covariation in the relative output of the underlying temporal channels at intermediate frequencies. Metha and Mullen (1996) proposed that the simplest model for this result is to assume that the [L - M] system is mediated by at least two bandpass temporal channels centered on approximately 2 and 8 Hz that overlap at intermediate temporal frequencies.

While discrimination is a useful technique for enumerating the underlying channels, it rests on certain assumptions that make it difficult to unambiguously differentiate between channel amplitude, peak location, and bandwidth. According to the standard ratio model of temporal frequency discrimination, thresholds will be minimal at temporal frequencies associated with greatest slope (i.e., change in amplitude as a function of temporal frequency) in channel response. However, channel slopes are determined by both the bandwidth and amplitude of their responses. Therefore, estimates of channel bandwidth, location, and amplitude based on discrimination performance alone potentially confound these factors. The present study uses an alternative technique, known as overlay masking, to estimate the number, temporal location, and shape of temporal channels within achromatic and each iso-luminant axis of human color space that rests on a different set of assumptions to estimates based on temporal frequency discrimination performance.

## Temporal masking within cardinal color axes

As mentioned above, masking studies indicate that luminance-driven vision is mediated by multiple temporal frequency channels: one low-pass and one (or two) bandpass channels (Anderson & Burr, 1985; Cass & Alais, 2006; Hess & Snowden, 1992; Lehky, 1985; Snowden & Hess, 1992). Temporal masking estimates the response profiles of the underlying psychophysical temporal frequency mechanisms by systematically measuring the extent to which sensitivity to a particular target frequency is corrupted by the superposition of an

irrelevant masking stimulus of variable temporal frequency. Psychophysical temporal overlay masking performance (threshold elevation) as it occurs as a function of masking contrast (known as the TvC function) implies the existence of at least two distinct components. These may be characterized as one that is approximately linear and orientation tuned and one that is non-linear (divisive), isotropic, and optimized to low spatial and high temporal frequencies (Cass & Alais, 2006; Medina & Mullen, 2009; Meese & Holmes, 2007). It is convenient to conceptualize masking as a reduction in the signal-to-noise ratio of a target-relevant channel response. According to the simple linear model, if the masking stimulus falls within the bandwidth of the target-relevant frequency's channel it will cause an increase in the relevant channel's output. This is equivalent to decreasing the channel's signal-to-noise ratio relative to the target-only response and is assumed to result in a reduction in target detectability (i.e., an increase in detection threshold). As the temporal frequency of the masking stimulus shifts away from the target-relevant channel's peak temporal frequency sensitivity (eventually falling beyond its bandwidth), signal-to-noise ratios are expected to increase, with a consequent improvement in detection performance. By systematically varying the temporal frequency of the masking stimulus relative to the target frequency and analyzing the concomitant rise and fall of detection performance, one can estimate the number, shape, and locations of the underlying temporal channels.

In addition to this approximately linear pooling of signal and noise, a non-linear, divisive masking component has been observed both psychophysically and neurophysiologically in cat area V1 to be invariant to orientation and selective for low spatial and high temporal frequencies (Bonds, 1989; Boynton & Foley, 1999; Cass & Alais, 2006; DeAngelis, Robson, Ohzawa, & Freeman, 1992; Medina & Mullen, 2009; Meese & Holmes, 2007; Meier & Carandini, 2002). While the source of this divisive masking component is unknown (e.g., suppression, ionic depression, decorrelating noise), functionally its effect can also be described in terms of variation in signal-to-noise ratio of the target-relevant channel. Therefore, temporal channel estimates based on masking are likely to represent some proportion of this isotropic masking component (Cass & Alais, 2006).

In this experiment, we use an equivalent temporal frequency masking paradigm (with 1- and 10-Hz targets) employed previously in the luminance domain to derive temporal channels along each of the axes of MBDKL space: achromatic [L + M + S]; S-cone isolating violet-yellow [S + S-]; and red-green [L - M]. If the iso-luminant system is mediated by a single low-pass mechanism (Burr & Morrone, 1993; Kulikowski, Robson, & McKeefry, 1996; Lee, Martin, & Valberg, 1989; McKeefry, Murray, & Kulikowski, 2001), we predict: (i) evidence for a low-pass masking function derived from 1-Hz detection performance; and (ii) no evidence for a more transient bandpass

red–green axes of MBDKL space. Conversely, if chromatically defined vision is mediated by multiple temporal frequency mechanisms, as suggested by temporal frequency discrimination performance in the [L – M] axis (Metha & Mullen, 1996; also see Cropper, 1994 for speed discrimination performance), then we should find evidence for two distinct yet overlapping temporal masking functions defined along each of the axes of MBDKL space.

## Temporal masking between cardinal color axes

In addition to mapping the structure of temporal channels using target and masking stimuli defined within each cardinal chromatic and achromatic axis of MBDKL space, we will examine temporal masking interactions between each of these axes. Our motivation for this between-axis examination is twofold. Our first motivation relates to the paucity of neurophysiological evidence as to the temporal tuning characteristics of chromatically driven cortical neurons. In the event that we do observe masking interactions between different cardinal color axes, an examination of the temporal tuning properties of these interactions will enable us to generate cortical physiological predictions that are functionally informed by human psychophysics. Secondly, in the event that masking effects observed within cardinal iso-luminant axes indicate the presence of temporal frequency-specific channels (low pass and/or bandpass) by measuring the extent to which these channels are evident when measured between iso-luminant cardinal axes will enable us to determine whether these channels are mediated at precortical or cortical loci.

This question is prompted by our earlier result showing dissociable orientation tuning for low and high temporal frequency masking (Cass & Alais, <u>2006</u>). Specifically, whereas low-pass masking functions are contingent upon the target and masks possessing similar orientations, transient bandpass masking functions appear to be comparatively less tuned for orientation.

Given that strong orientation selectivity does not emerge in the primate visual system until primary visual cortex (De Valois, Yund, & Hepler, 1982; Hubel & Wiesel, 1968; Schiller, Finlay, & Volman, 1976), this dissociation in orientation selectivity and temporal masking suggests that the low-pass masking effects may be cortically mediated, as opposed to the high bandpass effects, which may be precortical in origin. By analogy, if transient masking is indeed precortical and low-pass masking is cortical in origin, then we predict evidence for low-pass masking, but not the more bandpass transient masking function, in the context of targets and masks presented along the different iso-luminant axes of MBDKL space. If, however, transient masking does involve cortical interactions, then we expect to see evidence for it with targets and masks defined along different iso-luminant cardinal color axes [L – M] and [S + S–]. If the high temporal frequency channel is mediated precortically: as suggested by the orientation invariance of the

high temporal frequency masking function (Cass & Alais, <u>2006</u>); and the low temporal frequency channel is cortically mediated; as implied by the orientation dependence of the low temporal frequency masking function; then there should be no bandpass masking of high temporal frequency targets between cardinal color axes but should allow for masking of low temporal frequency targets between cardinal colors.

## Methods

#### **Observers**

Three normally sighted subjects aged 22–34 participated in the study. One subject (author JC) was a highly trained psychophysical observer and was aware of the study's hypotheses. The other subjects had minimal psychophysical experience and were naive to the purposes of the study.

### Materials

Stimuli were displayed on a Sony Trinitron G520 monitor operating at 100 Hz with a pixel resolution of  $1024 \times 768$  and were predrawn using a VSG 2/5 graphics card (Cambridge Research Systems, Kent, UK), which provides over 14 bits of contrast resolution per color channel, controlled by a PC. A mean luminance of 63.3 cd m $^{-2}$  was maintained throughout the experimental sessions in an otherwise dark environment. Viewing distance was fixed at 57 cm. Responses were registered by depressing one of two buttons located on a response box. The luminance output of each of the three phosphor guns was measured, calibrated, and linearized with an OptiCal photometer in conjunction with VSG 2/5 calibration software. Smith and Pokorny fundamentals were used to transform R, G, and B phosphor contrasts to L-, M-, and S-

cone contrasts. Phosphor chromaticities were: x = 0.61, y = 0.34 (red gun); x = 0.28, y = 0.594 (green gun); and x = 0.141, y = 0.070 (blue gun). For the S-cone isolating stimulus, the maximum S-cone contrast modulation was 87.3%. For the L – M stimulus, the maximum contrast was 7.7% for the L-cone modulation, and 12.3% for the M-cone modulation.

## Stimuli and procedures

Mask and target stimuli were vertical counterphasing gratings presented within a fixation-centered aperture subtending 10 degrees of visual angle against a gray background. Target and mask stimuli modulated sinusoidally across both space and time within either the achromatic [L + M + S] or one of the cardinal iso-luminant dimensions (L – M or S-cone isolating S + S $^-$ ) of the MBDKL space. The frequency of spatial modulation was held constant at 1 cycle per degree of visual angle. The temporal frequency of target and mask stimuli varied independently across stimulus conditions. In contexts in which target and masking stimuli were spatially and

temporally superimposed, spatial zero crossings were aligned. Temporal phase varied randomly across trials. Each stimulus interval was 1 s in duration with a 50-ms raised cosine ramp at onset and offset. All stimuli were viewed binocularly.

Each experiment consisted of three phases. The first phase involved establishing the point of subjective iso-luminance for chromatically defined stimuli. This was done using the minimum motion technique (Anstis & Cavanagh,  $\underline{1983}$ ) in both L – M and S – (L + M) dimensions. The point of subjective iso-luminance is known to vary substantially across the temporal frequency spectrum (Logothetis & Charles,  $\underline{1990}$ ; Metha & Mullen,  $\underline{1996}$ ). To control for this, on each day of testing, prior to threshold measurements (see below), the point of subjective iso-luminance was measured for each chromatic axis at temporal modulation rates equal to those used in subsequent threshold measurements. These values were then used to define target and masking stimuli throughout that day of testing. S-cone isolation was approximated for each subject following the minimum motion estimate described above (which was based on an equal proportion of L- and M-cone contrasts) by varying the proportion of L:M components of a static S – (L + M)-defined grating (1 c.p.d.) held at full contrast until minimum perceived contrast was attained.

The second phase of testing involved measuring contrast detection thresholds for target stimuli (achromatic [L + M + S], red–green [L - M], and S-cone isolating violet–yellow [S + S -]) at various temporal frequencies. Contrast detection thresholds were measured using a Bayesian adaptive two-interval forced-choice procedure, tracking detection performance at 81.6% correct

(Kontsevich & Tyler, <u>1999</u>). The results of this procedure are shown in <u>Figure 1</u>. The target was randomly presented in one of the two test intervals on each trial. The observers' task was to identify which test interval contained the target. Responses were registered using one of two buttons representing each test interval. Each threshold measurement was derived from 80 trials and was repeated four times. The chromaticity and temporal frequency of the target was kept constant throughout each threshold measurement.

The third experimental phase involved the detection of target stimuli presented at 4 dB above detection threshold whose look-up tables were then linearly added to those defining a given masking stimulus. The contrast of the masking stimulus varied systematically from trial to trial (Cass & Alais, 2006; Hess & Snowden, 1992; Snowden & Hess, 1992) under the control of the adaptive staircase, such that correct detection of target stimuli resulted in increased mask contrast, with incorrect detection resulting in decreased mask contrast, again converging on 81.6% correct performance. In this experimental phase, thresholds were measured using targets modulating at 1 and 10 Hz. Each target threshold was measured in the context of

multiple masking frequencies within the range of 1 to 30 Hz. Target and masking stimuli were each presented along either the same different axes of MBDKL space, producing a total of nine conditions, being the factorial combination of three targets ([L + M + S], [L - M], and [S + S - ]) and three masks ([L + M + S], [L - M], and [S + S - ]).

## Results

Our goal was to determine how sensitivity to target stimuli is affected by the temporal rate of masking stimuli defined either along the same or a different cardinal axis to that of the target. For each observer, we first estimated contrast detection thresholds for 1- and 10-Hz targets defined along each cardinal axis. These threshold estimates can be seen in <u>Table 1</u>. We then converted these threshold estimates to decibels using the following formula:

$$dB_{target} = 20 \times \log 10(T_{target}),$$
(1)

where  $T_{\text{target}}$  = target threshold expressed as a proportion of maximum contrast obtainable.

### Table 1

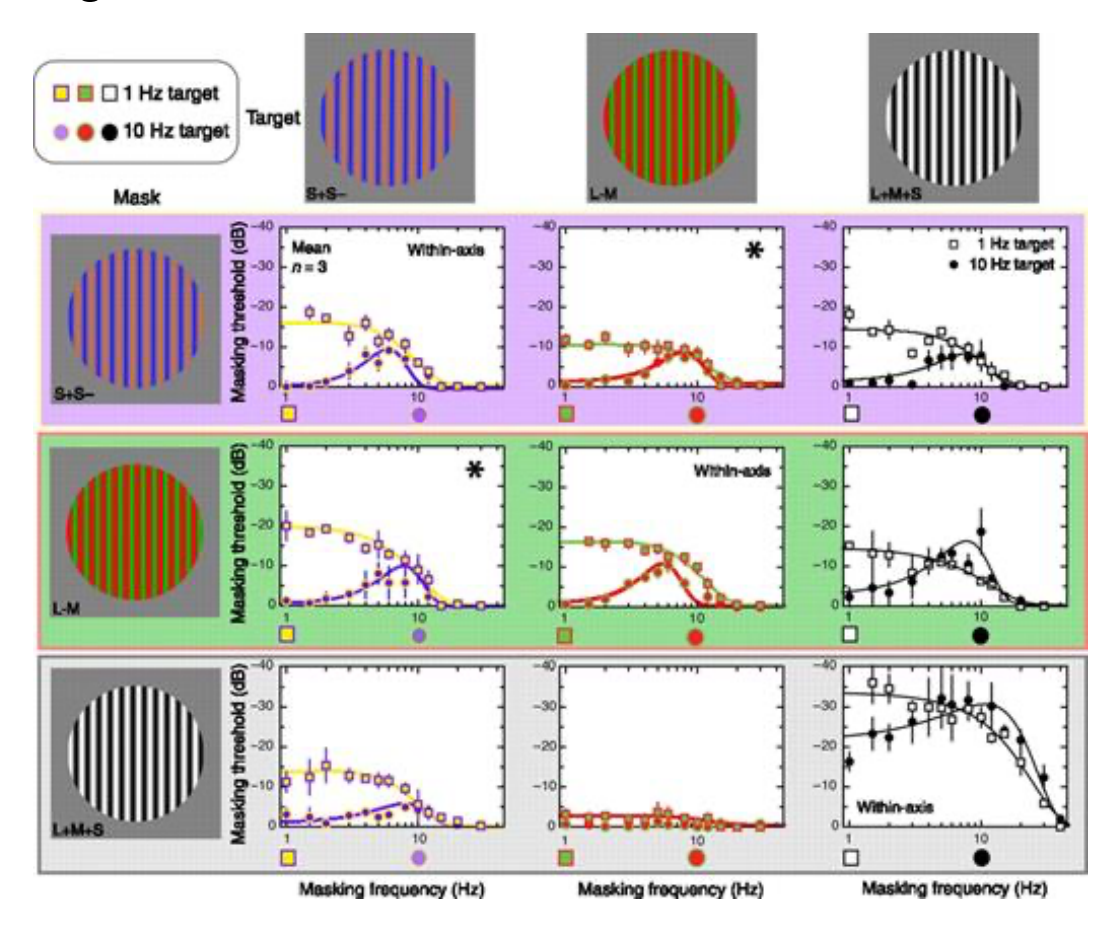


#### **View Table**

4- and 10-Hz target detection thresholds (raw contrast values) measured along each cardinal chromatic and achromatic axis for each observer.

In the masking phase of the experiment, target contrasts were fixed at 4 dB above target threshold estimates and masking contrasts were varied across trials. Each graph in <u>Figure 2</u> describes the extent to which target detection performance depended upon mask contrast, averaged over three observers. Individual subjects' data are shown in <u>Figure 3</u>. The ordinate in each individual graph (masking threshold) represents the mask contrast at which subjects achieved 82% target detection performance. Values closer to zero imply that detection performance was less affected by mask contrast (lower masking thresholds) than more negative values, which correspond to lower mask contrasts (higher masking thresholds).

Figure 2



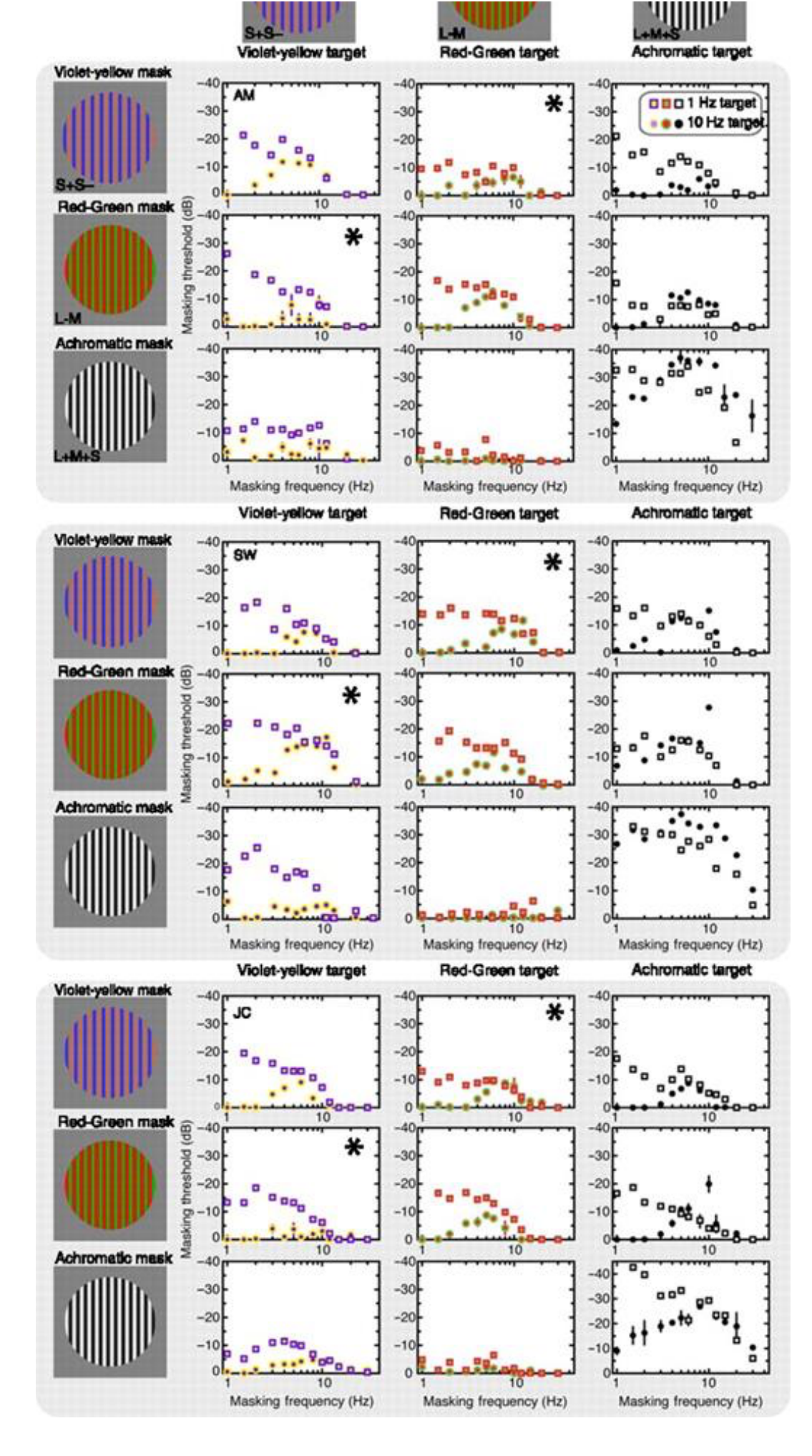
#### <u>View Original</u> <u>Download Slide</u>

Effects of temporal masking measured within and between cardinal color axes averaged across three different observers (individual observers' data are shown in Figure 3). The cardinal axes along which target and masking stimuli are defined are represented as columns and rows, respectively. Asterisks signify contexts in which target and masking stimuli are defined along different cardinal iso-luminant axes. The ordinate in each graph indicates the contrast of the masking stimulus generating target detection threshold performance. Target contrasts were fixed at 4 dB above unmasked detection threshold. More negative ordinate values (i.e., higher on the axis) indicate that threshold performance resulted at lower masking contrasts (indicating stronger masking) than less negative values. The abscissa in each graph represents the temporal frequency of the masking stimulus. Square and circle symbols indicate masking thresholds measured using 1- and 10-Hz targets, respectively. Error bars represent standard errors measured between subjects.

## Figure 3







Temporal masking for three different observers (each  $3 \times 3$  matrix represents a different subject's data) measured within cardinal color axes (top left, center, and bottom right) and between cardinal color axes. Error bars represent the standard error of between two and six separate threshold estimates. See <u>Figure 2</u> legend for more details.

The maximum contrast obtainable within each cardinal axis was limited by our equipment. Therefore, we could not exceed the maximum contrast of our masking stimuli, which decreased as target contrast increased. Any differences in target detection threshold (across color and temporal frequency) resulted in concomitant differences in the maximum possible masking contrast. To account for such differences, we normalized masking thresholds by expressing these values as a proportion of the maximum contrast obtainable for a given target threshold value:

$$dB_{\text{masking}} = 20 \times \log 10 (T_{\text{mask}}/C_{\text{max}}),$$

(2)

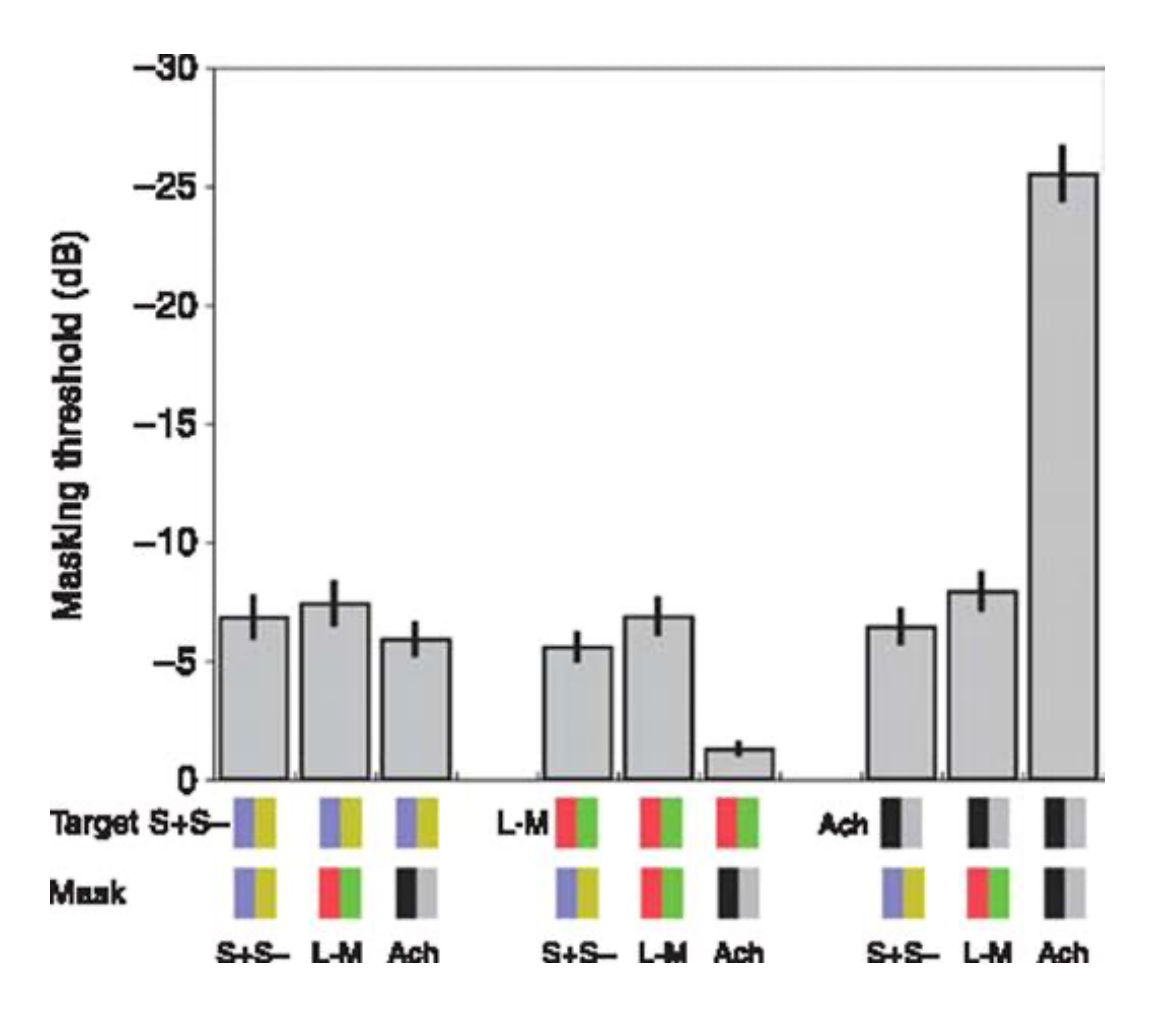
where  $T_{\text{mask}}$  = target threshold expressed as a proportion of full contrast, and  $C_{\text{max}}$  = maximum contrast obtainable = 1 –  $T_{\text{target}}$ .

The abscissa in each graph depicts the temporal frequency of the masking stimulus. Square and circular symbols represent the masking effects associated with 1- and 10-Hz targets, respectively. Figures 2 and 3 are each composed of nine separate graphs with columns representing targets defined within a given cardinal axis ([S + S -], [L - M], [L + M + S]) and rows, the cardinal axis defining a given masking stimulus. Top-left, center, and bottom-right graphs describe masking functions with targets and masks defined within the same cardinal axis. All other graphs describe between-cardinal axis masking effects. Iso-luminant between-axis interactions (denoted by asterisks) are represented by center-top and center-left masking functions.

### Within cardinal axis effects

As can be seen in <u>Figures 2</u> and <u>3</u>, elevations in masking thresholds (i.e., more negative ordinate values) are observed when both target and masking stimuli are defined along the same direction of the color space ([L + M + S], [L - M], or [S + S -]). Collapsed across temporal frequency, two separate within-subjects *t*-tests reveal that the magnitude of threshold elevation observed in the achromatic axis greatly exceeds that observed in either iso-luminant axis (both *p*-values < 0.001; see <u>Figure 4</u>).

Figure 4



View Original Download Slide

Effects of temporal masking collapsed across temporal frequency, measured within and between cardinal color axes and averaged across three different observers. Error bars represent standard errors measured between subjects.

Qualitatively equivalent patterns of masking are observed as a function of temporal frequency

in both iso-luminant and achromatic directions. Robust threshold elevations are observed for 1-Hz targets when presented in the context of masking frequencies < ~10 Hz and are well fitted by a broad Gaussian function centered at 0.1 Hz. This low-pass masking behavior is distinguishable from that derived using 10-Hz targets, which exhibit maximum threshold elevation between ~5 and 10 Hz. These 10-Hz target masking functions are well fitted by a comparatively narrowband Gaussian function centered between 7 and 12 Hz.

#### Between cardinal color axis effects

As can be seen in <u>Figures 2</u> and <u>3</u>, generally speaking target stimuli defined within a given cardinal axis are robustly masked by stimuli defined along a different cardinal axis. These instances of masking are well fitted by a combination of a low-pass and a more transient

bandpass Gaussian function ( Figure 2). The single exception to these strong between-axis masking effects can be observed in the case of targets defined along the [L - M] axis masked by stimuli defined along the achromatic [L + M + S] axis. This apparent insusceptibility of [L - M]-defined target detection performance to achromatic masking is asymmetric as achromatic targets are robustly masked by stimuli defined along the [L - M] axis. Collapsing across temporal frequency, a within-subjects analysis of variance reveals that, with this one exception, masking thresholds do not vary significantly when target and/or masking stimuli are defined along at least one iso-luminant cardinal color axis. In the case of red–green targets and achromatic masks we find significantly smaller threshold elevations (p < 0.01; see Figure 4).

# Discussion

We find that target and masking stimuli defined along each cardinal iso-luminant axis ([L – M] and S-cone isolating [S + S–]) produce the classic low-pass and higher bandpass temporal masking functions previously observed using luminance-defined stimuli (Anderson & Burr, 1985; Cass & Alais, 2006; Hess & Snowden, 1992; Lehky, 1985; Snowden & Hess, 1992; see Figure 2). This finding challenges early temporal characterizations of iso-luminant psychophysical response: namely that chromatic stimuli are mediated by a single low-pass temporal mechanism (Burr & Morrone, 1993; Kulikowski et al., 1996; Lee et al., 1989; McKeefry et al., 2001). That our masking results indicate the presence of at least two overlapping, iso-luminant temporal channels peaking at <2 Hz and >6 Hz strongly supports the conclusions of Metha and Mullen (1996) based on temporal frequency discrimination performance defined along the L – M axis. Given that we find a similar pattern of masking in both L – M and S + S–axes, we predict that temporal frequency discrimination performance would be similar along both iso-luminant cardinal axes.

Despite the qualitative similarity between the luminance- and chromatically defined masking

functions, some differences are observed. Luminance-driven temporal masking functions reveal an average transient bandpass function peaking at ~10 Hz. Chromatically defined (red-green and yellow-violet) transient masking functions peak at lower temporal frequencies (~6 Hz). Additionally, whereas the amplitude of luminance-derived transient channel is at least as high as the low-pass channel at high temporal frequencies, for chromatically defined stimuli, the more transient channel tends to be relatively lower in amplitude above 5 Hz and have lower high frequency cutoffs (~10 Hz for red–green and yellow–violet; ~30 Hz for luminance). The combination of these factors suggests that although both chromatic and luminance systems possess multiple temporal frequency channels, compared with the luminance system, the chromatic transient channel appears to be comparatively less prominent. This may explain the various phenomenological differences in chromatic and luminance temporal vision that have previously been put forth as support for the idea that chromatic vision is mediated by a single low-pass mechanism, including: chromatic slowing (Mullen & Boulton, 1992); lower critical flicker fusion limits for chromatically defined stimuli; and the low-pass shape of both the chromatically defined MTF (Burr & Morrone, 1993; Lee et al., 1989; McKeefry et al., 2001) and Fourier transformed IRFs (Burr & Morrone, 1993).

Our psychophysical evidence for multiple temporal frequency channels is echoed in the results of several studies involving objective measurement of visually driven human cortical response. Cortically generated magnetic field responses (measured using the magnetocephalograph (MEG)) show a multimodal distribution when measured as a function of stimulus flicker rate. These are particularly prominent for stimulus modulations of: 0.1 and 4 Hz for red-green flicker (Fylan, Holliday, Singh, Anderson, & Harding, 1997); and ~2 and 8 Hz for luminance flicker (Fylan et al., <u>1997</u>; Muthukumaraswamy & Singh, <u>2008</u>). Other measures of human cortical response (visually evoked scalp potentials (VEP)), however, tend to show a unimodal peak in stimulusdependent cortical activity ~4 Hz (Crognale, Switkes, & Adams, 1997; Morrone, Fiorentini, & Burr, 1996; Rabin, Switkes, Crognale, Schneck, & Adams, 1994) in response to red-green and yellow-violet flickers. This result may be contrasted with that of Kulikowski et al. (1996) who found low-pass chromatically driven VEPs, and Morrone et al. (1996) who found a second peak at 10 Hz when using low spatial frequencies (0.3 c.p.d) in the red-green axis. Most luminancedriven studies of human cortical response fail to provide evidence for a distinct low-pass temporal frequency response component. Instead VEP, MEG, and metabolically sensitive measures (including Positron Emission Tomography (PET) and functional Magnetic Resonance Imaging (fMRI)) typically show a strong unimodal peak at 8–10 Hz (PET: Fox & Raichle, 1985; Vafaee et al., 1999; fMRI: Kaufmann, Elbel, Gössl, Pütz, & Auer, 2001; Kwong et al., 1992; Muthukumaraswamy & Singh, 2008; Singh, Smith, & Greenlee, 2000; MEG: Fawcett, Barnes, Hillebrand, & Singh, 2004; VEP: Morrone et al., 1996; Singh, Kim, & Kim, 2003).

If the human cortex does possess multiple temporal frequency channels, why do most (but not all; Fylan et al., 1997; Muthukumaraswamy & Singh, 2008) objective measures fail to register them? One possibility may be that what appears to be a unimodal peak in cortical activity may actually represent the combined activity of multiple channels. This is analogous to the suggestion that the psychophysical MTF fails to differentiate the output of the underlying channels (Robson, 1966) derived using masking (Anderson & Burr, 1985; Cass & Alais, 2006;

Hess & Snowden, 1992; Lehky, 1985; Snowden & Hess, 1992), adaptation (Langley & Bex, 2007), and temporal frequency discrimination (Metha & Mullen, 1996, 1997; Waugh & Hess, 1994). This idea receives support from a recent study in which the topography of human primary visual cortical BOLD signals was found to selectively differentiate between 1- and 15-Hz luminance flicker (Sun et al., 2007). Not only does this result support the idea that human primary visual cortex possesses distinct temporal frequency channels, but these channels may not always be derivable from simple MTFs, be they psychophysical or neurophysiological in their measurement.

What do we know of the temporal frequency response of single neurons along each of the axes of MBDKL space? In addition to chromatic selectivity, early visual neurons generate their own MTF. That is, they respond preferentially to different rates of temporal modulation. The MTFs of each of the axes of MBDKL space have been well documented in primate retina and lateral geniculate nucleus. These are typically characterized as bandpass with peak responses occurring at approximately 10 Hz (Lee et al., 1989; Lee, Pokorny, Smith, Martin, & Valberg, 1990; Lennie et al., 1990; Solomon, White, & Martin, 1999), although other retinal cells, such as bipolar neurons, are more low pass (Burkhardt, Fahey, & Sikora, 2007). Our understanding of how these early temporal response properties are transferred to the cortex is less clear, however. In the case of luminance-defined stimulation, cortical neurons generally respond with lower peak sensitivities and high frequency cutoffs compared with precortical neurons. While this suggests that a significant amount of temporal information may be lost as a consequence of the thalamo-cortical transformation, macaque cortical neurons actually exhibit considerable diversity in their temporal tuning, ranging from low pass to low and high bandpass, with neural responses to stimulus temporal frequencies peaking between 3 and 8 Hz (V1: Foster, Gaska, Nagler, & Pollen, 1985; Hawken, Shapley, & Grosof, 1996; Zheng et al., 2007; V2: Levitt, Kiper, & Movshon, 1994; Mareschal & Baker, 1998; V3: Gegenfurtner, Kiper, & Levitt, 1997; MT: Lui, Bourne, & Rosa, 2007; Priebe, Cassanello, & Lisberger, 2003), slightly lower, on average, than found in most human imaging studies (see above). Despite this rather substantial physiological literature on the responsiveness of cortical neurons to different luminance-defined temporal frequencies, relatively little is known about the temporal transfer properties of chromatically

driven cortical neurons.

Our evidence for both low-pass and high bandpass masking functions between chromatic axes (red-green target/yellow-violet mask; yellow-violet target/red-green mask) implies that both low-pass and high bandpass channels are the result of activity at a level of the visual processing

hierarchy that receives input across cardinal iso-luminant dimensions. Neurophysiological evidence indicates that in the primate visual system such inter-cardinal chromatic axis interactions are not observed until primary visual cortex (Cottaris & De Valois, 1998; Derrington et al., 1984; Lennie et al., 1990). Our results indicate, therefore, that at least in the context of interactions between iso-oriented targets and masks defined along different axes of MBDKL space, both low-pass and high bandpass psychophysical temporal channels are likely to be mediated by cortical rather than purely subcortical mechanisms.

At first glance, the observation that a transient bandpass masking function is evident between the iso-luminant cardinal axes appears at odds with the findings of Cass and Alais (2006) who found that achromatically defined high bandpass temporal masking functions were orientation invariant, possibly suggesting a precortical locus (Freeman, Durand, Kiper, & Carandini, 2002; Li, Peterson, Thompson, Duong, & Freeman, 2005; Li, Thompson, Duong, Peterson, & Freeman, 2006). There may be several explanations for this apparent discrepancy. Firstly, transient masking may occur at multiple stages of visual processing. Dan, Atick, and Reid (1996) showed that transient luminance-driven masking of low temporal frequency responses (referred to as temporal decorrelation or "whitening") is evident in the spiking activity of cat LGN. A similarly asymmetric form of transient temporal masking is observed in cat V1 (Allison, Smith, & Bonds, 2001). Whether these instances of transient neural masking occur in response to iso-luminant stimuli is unknown.

A second possibility is that the high bandpass channel may be mediated by non-orientation-selective cortical neurons that receive input across cardinal axes. Neurons with both of these properties are found in the earliest primary visual cortical layers as well as the cytochrome oxidase-rich "blob" and "stripe" regions of primate V1 and V2, respectively (Lu & Roe, 2008). In a recent psychophysical study, Medina and Mullen (2009) showed that iso-luminant [L – M]-defined masking (of L – M targets) is orientation invariant across a broad range of spatio-temporal frequencies. This is to be distinguished from achromatic masking in which the high bandpass masking component, but not the low-pass component, is orientation invariant (Cass & Alais, 2006). The combination of these results suggests that while achromatic and iso-luminant low-pass masking effects may be mediated by different sets of mechanisms, high bandpass masking may result from non-orientation- and non-color-selective intra-cortical or

cortico-thalamic interactions. Despite the paucity of electrophysiological evidence regarding the temporal frequency tuning properties of chromatically selective cortical neurons, their functional predictions may be tested psychophysically by covarying the relative chromaticity,

luminance, orientation, and temporal frequency of target and masking stimuli.

A third possibility is the introduction of luminance artifacts in our ostensibly iso-luminant stimuli. Such luminance intrusions may occur for several reasons. For example, our estimates of S-cone isolation measured for each subject (using static gratings) may vary as a function at different rates of temporal modulation. Furthermore, the points of subjective iso-luminance measured for L – M and S-cone isolated pathways may vary when simultaneously stimulated by both axes (as occurs during between-axis iso-luminant masking). In the event that such luminance intrusions do occur, then any masking effects observed between iso-luminant axes may reflect contributions from the luminance pathway. To our knowledge, neither of these temporal frequency contingencies have been tested psychophysically, and therefore, we must reserve caution in interpreting our iso-luminant masking effects. One reason to suspect that our iso-luminant effects are not a consequence of luminance-driven intrusions is our observation that achromatic (luminance-defined) masks induce very little threshold elevation for [L - M]defined targets at any temporal frequency (see below). This implies that the threshold elevations observed for [L - M]-defined targets in the context of [S + S-]-defined masks were not due to the presence of luminance artifacts. Nonetheless, future research is needed to determine the validity of this inference.

In addition to the robust masking that occurs within and between each cardinal direction of color space, we observe an interesting asymmetry between red–green and achromatic axes. To summarize this effect: no matter how much achromatic noise we added, subjects were able to reliably detect low contrast red–green targets. This is contrasted with the finding that achromatically defined target thresholds are robustly increased by the presence of red–green masks. This asymmetry has been reported previously using non-dynamic masking (Gegenfurtner & Kiper, 1992; Li & Lennie, 1997, 2001; Switkes, Bradley, & De Valois, 1988), although Vimal (1998) showed that the resistance of red–green targets to achromatic masks is restricted to spatial frequencies >0.125 c.p.d. At first glance, the fact that red–green contrast effectively masks achromatically defined targets appears to contradict the converse situation whereby achromatic masks had little or no deleterious effect on red–green target detection at any temporal frequency. This dissociation between the asymmetric masking effects observed between luminance and red–green axes implies that the luminance-sensitive detection mechanism receives red–green input but not vice versa. Other results are consistent with this conclusion but indicate that interactions between luminance and red–green are dependent on

task demands. For example, Yoshizawa, Mullen, and Baker (2003) showed that while red-green

motion direction discrimination was compromised by the presence of dynamic luminance noise, detection sensitivity was not (see also Cropper & Derrington, 1994). A similar conclusion was drawn by Willis and Anderson (2002) using an adaptation paradigm whereby prolonged viewing of a drifting luminance grating disrupted direction discrimination of a subsequently presented red–green grating but not its detectability.

This notion that luminance and red–green detection is mediated by a different relative combination of luminance and red–green input to that associated with perceived direction of motion is complicated by the finding that subthreshold summation (a detection task) between red–green and luminance indicates comparative independence between these cardinal color dimensions (Mullen, Cropper, & Losada, 1997). A possible explanation for the apparent discrepancy between subthreshold summation and masked detection performance may relate to differences in the contrast of the masking and summation stimuli used in these paradigms. Indeed, subthreshold summation and masking are in fact differentiated only by psychophysical performance, rather than stimulus or task. Low contrast masks are known to produce facilitation: the well-known dipper function (Boynton & Foley, 1999). Future research is required to determine the extent to which TvC functions vary as a function of temporal frequency (Boynton & Foley, 1999; Medina & Mullen, 2009) when target and masking stimuli are defined in different directions of color space.

It has been suggested that the phylogenic differentiation of L- and M-selective cones in primates may have evolved from selective pressures favoring the segregation of ripened fruit against foliage (Mollon, 1989). Our finding that red–green detection performance is relatively impervious to luminance masking is not inconsistent with this idea as it would seem advantageous that sources of illumination variation, due to shadow or aqueous refraction, should not mask the detection of food sources. Another functional explanation may relate to the observation that in natural scenes, red–green contrast reflectances tend not to vary significantly under different illumination conditions (Lovell et al., 2005). Given that naturally occurring red–green contrast and luminance information does not covary across time, it would seem reasonable that the visual system's functional organization should reflect this independence if it is to capitalize upon it. By contrast, naturally occurring yellow–violet reflectances are found to exhibit significant temporal correlations with luminance with such that shadows exhibit a greater proportion of short wavelengths (Lovell et al., 2005). This lack of naturally occurring independence between luminance and yellow–violet reflectance may serve to explain our finding that under a broad range of temporal conditions, our subjects failed to

differentiate luminance from yellow–violet. Based on these results, it seems reasonable to say that luminance resembles the yellow–violet dimension more so than it does the red–green dimension.

# Conclusions

Using a classical psychophysical masking paradigm, we have estimated the number, bandwidth, and peak selectivity of temporal channels in each of the cardinal iso-luminant and achromatic axes of MBDKL space. We find that a qualitatively similar pattern of temporal masking is observed using target and masking stimuli defined within each cardinal color axis (Experiment 1). These patterns may be characterized as two distinct functions: one low-pass and one that is high frequency-selective and bandpass (derived using 1- and 10-Hz targets, respectively). That both low-pass and higher bandpass masking functions are observed in response to stimuli defined along each iso-luminant cardinal axis (yellow-violet and red-green) supports and extends upon the findings of previous studies involving objective measurement of human cortical activity (Fylan et al., 1997; Morrone et al., 1996; Muthukumaraswamy & Singh, 2008; Sun et al., 2007) and psychophysical response (Metha & Mullen, 1996; Waugh & Hess, 1994), which suggest that both luminance- and iso-luminant [L – M]-driven systems are mediated by multiple temporal frequency channels. Our finding that both temporal channels are evident in each iso-luminant cardinal axis predicts that the results of these earlier discrimination and imaging studies should generalize to the S-cone isolating pathway.

Somewhat surprisingly, we have also found that for the most part, targets and masks defined along different cardinal axes generate similar masking functions to those found within each axis (see Figures 2 and 3). That both low-pass and bandpass temporal masking functions are evident between iso-luminant axes indicates that both temporal channels may be mediated by cortical mechanisms (Cottaris & De Valois, 1998; Derrington et al., 1984; Lennie et al., 1990). In an earlier study (Cass & Alais, 2006), we found that the low-pass but not the bandpass temporal masking function depended strongly on the relative orientation of target and mask. This difference in orientation selectivity of sustained and transient masking suggested that transient and sustained channels were mediated by precortical and cortical mechanisms, respectively. The results of our current study indicate that both sustained (low-pass) and transient (bandpass) masking effects transfer between iso-luminant color axes, suggesting the involvement of interactions within either the earliest cortical layers (IVa and IVc) and/or the cytochrome oxidase-rich regions such as the "blobs" and "stripes" found in V1 and V2 (Livingstone & Hubel, 1984; Lu & Roe, 2008; Ts'o & Gilbert, 1988). Alternatively, the between-axis chromatic masking effects we observe could conceivably be a consequence of non-specific interactions between orientation-selective and/or chromatically selective cells within V1 (Heeger, 1992).

-

An exception to the general finding of threshold elevation when targets and masks are defined along different cardinal axes is observed in the case of red–green targets and achromatically defined masks. This result extends previous findings that red–green detection performance is relatively impervious to achromatic masking by showing that this effect persists across different temporal frequencies (Gegenfurtner & Kiper, 1992; Li & Lennie, 1997, 2001; Switkes et al., 1988; Vimal, 1998). That this chromatic effect is asymmetric (i.e., achromatically defined targets are robustly masked by red–green masks according to the standard low-pass/high bandpass temporal masking profile) suggests differential input properties for luminance and red–green detection mechanisms. The uniqueness of this interaction within the domain of MBDKL space suggests an important functional role, possibly to optimize fruit foraging under varying illumination conditions (Lovell et al., 2005; Mollon, 1989).

# Acknowledgments

This research was supported by grants awarded to John Cass (DP0774697) and Branka Spehar (DP0345612) by the Australian Research Council. We wish to thank Samuel Solomon for colorful and illuminating discussion.

Commercial relationships: none.

Corresponding author: John Cass.

Email: johncassvision@gmail.com.

Address: School of Psychology, University of Sydney, Sydney, NSW 2006, Australia.

# References

Allison, J. D. Smith, K. R. Bonds, A. B. (2001). Temporal-frequency tuning of cross-orientation suppression in the cat striate cortex. Visual Neuroscience, 18, 941–948. [PubMed] [PubMed]

Anderson, S. J. Burr, D. C. (1985). Spatial and temporal selectivity of the human motion detection system. Vision Research, 25, 1147–1154. [PubMed] [CrossRef] [PubMed]

Anstis, S. M. Cavanagh, P. Mollon, J. D. Sharpe, L. T. (1983). A minimum motion technique for judging equiluminance. Colour vision: Psycho-physics and physiology. (pp. 155–166). London: Academic Press.

Blakemore, C. Campbell, F. W. (1969a). Adaptation to spatial stimuli. The Journal of Physiology, 200, 11PBlakemore, C., & Campbell, F. W. (1969a). Adaptation to spatial stimuli. *The Journal of Physiology, 200,* 11P–13P. [PubMed]

Riakamara, C. Camphall, E. W. (1969b). On the existence of neurones in the human visual system selectively

sensitive to the orientation and size of retinal images. The Journal of Physiology, 203, 237–260. [PubMed]

[Article] [CrossRef]

Bonds, A. B. (1989). Role of inhibition in the specification of orientation selectivity of cells in the cat striate cortex. Visual Neuroscience, 2, 41–55. [PubMed] [CrossRef] [PubMed]

Boynton, G. M. Foley, J. M. (1999). Temporal sensitivity of human luminance pattern mechanisms determined by masking with temporally modulated stimuli. Vision Research, 39, 1641–1656. [PubMed] [CrossRef] [PubMed]

Brown, P. K. Wald, G. (1963). Visual pigments in human and monkey retinas. Nature, 200, 37–43. [PubMed] [CrossRef] [PubMed]

Brown, P. K. Wald, G. (1964). Visual pigments in single rods and cones of the human retina Direct measurements reveal mechanisms of human night and color vision. Science, 144, 45–52. [PubMed] [PubMed]

Burkhardt, D. A. Fahey, P. K. Sikora, M. A. (2007). Retinal bipolar cells: Temporal filtering of signals from cone photoreceptors. Visual Neuroscience, 24, 765–774. [PubMed] [CrossRef] [PubMed]

Burr, D. C. Morrone, M. C. (1993). Impulse-response functions for chromatic and achromatic stimuli. Journal of the Optical Society of America, 10, 1706–1713. [CrossRef]

Burr, D. C. Morrone, M. C. (1996). Temporal impulse response functions for luminance and colour during saccades. Vision Research, 36, 2069–2078. [PubMed] [CrossRef] [PubMed]

Cass, J. Alais, D. (2006). Evidence for two interacting temporal channels in human visual processing. Vision Research, 46, 2859–2868. [PubMed] [CrossRef] [PubMed]

Cavanagh, P. Tyler, C. W. Favreau, O. E. (1984). Perceived velocity of moving chromatic gratings. Journal of the Optical Society of America A, Optics and Image Science, 1, 893–899. [PubMed] [CrossRef] [PubMed]

Cottaris, N. P. De Valois, R. L. (1998). Temporal dynamics of chromatic tuning in macaque primary visual cortex. Nature, 395, 896–900. [PubMed] [CrossRef] [PubMed]

Crognale, M. A. Switkes, E. Adams, A. J. (1997). Temporal response characteristics of the spatiochromatic visual evoked potential: Nonlinearities and departures from psychophysics. Journal of the Optical Society of America A, Optics, Image Science, and Vision, 14, 2595–2607. [PubMed] [CrossRef] [PubMed]

Cropper, S. J. (1994). Velocity discrimination in chromatic gratings and beats. Vision Research, 34, 41–48. [PubMed] [CrossRef] [PubMed]

Cropper, S. J. Derrington, A. M. (1994). Motion of chromatic stimuli: First-order or second-order? Vision Research, 34, 49–58. [PubMed] [CrossRef] [PubMed]

Dan, Y. Atick, J. J. Reid, R. C. (1996). Efficient coding of natural scenes in the lateral geniculate nucleus: Experimental test of a computational theory. Journal of Neuroscience, 16, 3351–3362. [PubMed] [PubMed]

Dartnall, H. J. Bowmaker, J. K. Mollon, J. D. (1983). Human visual pigments: Microspectrophotometric results from the eyes of seven persons. Proceedings of the Royal Society of London B: Biological Sciences, 220, 115–130. [PubMed] [CrossRef]

DeAngelis, G. C. Robson, J. G. Ohzawa, I. Freeman, R. D. (1992). Organization of suppression in receptive fields of neurons in cat visual cortex. Journal of Neurophysiology, 68, 144–163. [PubMed] [PubMed]

de Lange, H. (1958). Research into the dynamic nature of the human fovea–cortex systems with intermittent and modulated light I Attentuation characteristics with white and colored light. Journal of the Optical Society of America, 48, 777–784. [PubMed] [CrossRef] [PubMed]

De Monasterio, F. M. Gouras, P. (1975). Functional properties of ganglion cells of the rhesus monkey retina. The Journal Physiology, 251, 167–195. [PubMed] [Article] [CrossRef]

Derrington, A. M. Krauskopf, J. Lennie, P. (1984). Chromatic mechanisms in lateral geniculate nucleus of macaque. The Journal of Physiology, 357, 241–265. [PubMed] [Article] [CrossRef] [PubMed]

De Valois, R. L. Yund, E. W. Hepler, N. (1982). The orientation and direction selectivity of cells in macaque visual cortex. Vision Research, 22, 531–544. [PubMed] [CrossRef] [PubMed]

Eskew, Jr., R. T. Stromeyer, C. F. Kronauer, R. E. (1994). Temporal properties of the red–green chromatic mechanism. Vision Research, 34, 3127–3137. [PubMed] [CrossRef] [PubMed]

Fawcett, I. P. Barnes, G. R. Hillebrand, A. Singh, K. D. (2004). The temporal frequency tuning of human visual cortex investigated using synthetic aperture magnetometry. Neuroimage, 21, 1542–1553. [PubMed]

Foster, K. H. Gaska, J. P. Nagler, M. Pollen, D. A. (1985). Spatial and temporal frequency selectivity of neurones in visual cortical areas V1 and V2 of the macaque monkey. The Journal of Physiology, 365, 331–363. [PubMed] [Article] [CrossRef] [PubMed]

Fox, P. T. Raichle, M. E. (1985). Stimulus rate determines regional brain blood flow in striate cortex. Annals of Neurology, 17, 303–305. [PubMed] [CrossRef] [PubMed]

Freeman, T. C. Durand, S. Kiper, D. C. Carandini, M. (2002). Suppression without inhibition in visual cortex. Neuron, 35, 759–771. [PubMed] [Article] [CrossRef] [PubMed]

Fylan, F. Holliday, I. E. Singh, K. D. Anderson, S. J. Harding, G. F. (1997). Magnetoencephalographic investigation of human cortical area V1 using color stimuli. Neuroimage, 6, 47–57. [PubMed] [CrossRef]

#### [PubMed]

Gegenfurtner, K. R. Kiper, D. C. (1992). Contrast detection in luminance and chromatic noise. Journal of the Optical Society of America A, Optics and Image Science, 9, 1880–1888. [PubMed] [CrossRef] [PubMed]

Gegenfurtner, K. R. Kiper, D. C. Levitt, J. B. (1997). Functional properties of neurons in macaque area V3. Journal of Neurophysiology, 77, 1906–1923. [PubMed] [Article] [PubMed]

Hawken, M. J. Shapley, R. M. Grosof, D. H. (1996). Temporal-frequency selectivity in monkey visual cortex. Visual Neuroscience, 13, 477–492. [PubMed] [CrossRef] [PubMed]

Heeger, D. J. (1992). Normalization of cell responses in cat striate cortex. Visual Neuroscience, 9, 181–197. [PubMed] [CrossRef] [PubMed]

Hess, R. F. Snowden, R. J. (1992). Temporal properties of human visual filters: Number, shapes and spatial covariation. Vision Research, 32, 47–59. [PubMed] [CrossRef] [PubMed]

Hubel, D. H. Wiesel, T. N. (1968). Receptive fields and functional architecture of monkey striate cortex. The Journal of Physiology, 195, 215–243. [PubMed] [Article] [CrossRef] [PubMed]

Johnson, E. N. Hawken, M. J. Shapley, R. (2004). Cone inputs in macaque primary visual cortex. Journal of Neurophysiology, 91, 2501–2514. [PubMed] [Article] [CrossRef] [PubMed]

Kaufmann, C. Elbel, G. K. Gössl, C. Pütz, B. Auer, D. P. (2001). Frequency dependence and gender effects in visual cortical regions involved in temporal frequency dependent pattern processing. Human Brain Mapping, 14, 28–38. [PubMed] [CrossRef] [PubMed]

Kelly, D. H. (1983). Spatiotemporal variation of chromatic and achromatic contrast thresholds. Journal of the Optical Society of America, 73, 742–750. [PubMed] [CrossRef] [PubMed]

Kontsevich, L. L. Tyler, C. W. (1999). Bayesian adaptive estimation of psychometric slope and threshold. Vision Research, 39, 2729–2737. [PubMed] [CrossRef] [PubMed]

Kulikowski, J. J. Robson, A. G. McKeefry, D. J. (1996). Specificity and selectivity of chromatic visual evoked potentials. Vision Research, 36, 3397–3401. [PubMed] [CrossRef] [PubMed]

Kwong, K. K. Belliveau, J. W. Chesler, D. A. Goldberg, I. E. Weisskoff, R. M. Poncelet, B. P. (1992). Dynamic magnetic resonance imaging of human brain activity during primary sensory stimulation. Proceedings of the National Academy of Sciences of the United States of America, 89, 5675–5679. [PubMed] [Article] [CrossRef] [PubMed]

Langley, K. Bex, P. J. (2007). Contrast adaptation implies two spatiotemporal channels but three adapting processes. Journal of Experimental Psychology: Human Perception and Performance, 33, 1283–1296. [PubMed] [CrossRef] [PubMed]

Lee, B. B. Martin, P. R. Valberg, A. (1989). Sensitivity of macaque retinal ganglion cells to chromatic and

luminance flicker. The Journal of Physiology, 414, 223–243. [PubMed] [Article] [CrossRef] [PubMed]

Lee, B. B. Pokorny, J. Smith, V. C. Martin, P. R. Valberg, A. (1990). Luminance and chromatic modulation sensitivity of macaque ganglion cells and human observers. Journal of the Optical Society of America A, Optics and Image Science, 7, 2223–2236. [PubMed] [CrossRef] [PubMed]

Lehky, S. R. (1985). Temporal properties of visual channels measured by masking. Journal of the Optical Society of America A, Optics and Image Science, 2, 1260–1272. [PubMed] [CrossRef] [PubMed]

Lennie, P. Krauskopf, J. Sclar, G. (1990). Chromatic mechanisms in striate cortex of macaque. Journal of Neuroscience, 10, 649–669. [PubMed] [Article] [PubMed]

- Levitt, J. B. Kiper, D. C. Movshon, J. A. (1994). Receptive fields and functional architecture of macaque V2. Journal of Neurophysiology, 71, 2517–2542. [PubMed] [PubMed]
- Li, A. Lennie, P. (1997). Mechanisms underlying segmentation of colored textures. Vision Research, 37, 83–97. [PubMed] [CrossRef] [PubMed]
- Li, A. Lennie, P. (2001). Importance of color in the segmentation of variegated surfaces. Journal of the Optical Society of America A, Optics, Image Science, and Vision, 18, 1240–1251. [PubMed] [CrossRef] [PubMed]
- Li, B. Peterson, M. R. Thompson, J. K. Duong, T. Freeman, R. D. (2005). Cross-orientation suppression: Monoptic and dichoptic mechanisms are different. Journal of Neurophysiology, 94, 1645–1650. [PubMed] [Article] [CrossRef] [PubMed]
- Li, B. Thompson, J. K. Duong, T. Peterson, M. R. Freeman, R. D. (2006). Origins of cross-orientation suppression in the visual cortex. Journal of Neurophysiology, 96, 1755–1764. [PubMed] [Article] [CrossRef] [PubMed]
- Livingstone, M. S. Hubel, D. H. (1984). Anatomy and physiology of a color system in the primate visual cortex. Journal of Neuroscience, 4, 309–356. [PubMed] [Article] [PubMed]
- Logothetis, N. K. Charles, E. R. (1990). The minimum motion technique applied to determine isoluminance in psychophysical experiments with monkeys. Vision Research, 30, 829–838. [PubMed] [CrossRef] [PubMed]
- Lovell, P. G. Tolhurst, D. J. Párraga, C. A. Baddeley, R. Leonards, U. Troscianko, J. (2005). Stability of the color-opponent signals under changes of illuminant in natural scenes. Journal of the Optical Society of America A, Optics, Image Science, and Vision, 22, 2060–2071. [PubMed] [CrossRef] [PubMed]
- Lu, H. D. Roe, A. W. (2008). Functional organization of color domains in V1 and V2 of macaque monkey revealed by optical imaging. Cerebral Cortex, 18, 516–533. [PubMed] [Article] [CrossRef] [PubMed]
- Lui, L. L. Bourne, J. A. Rosa, M. G. (2007). Spatial and temporal frequency selectivity of neurons in the middle temporal visual area of new world monkeys (Callithrix jacchus. European Journal of Neuroscience, 25, 1780–1792. [PubMed] [CrossRef] [PubMed]
- MacLeod, D. I. Boynton, R. M. (1979). Chromaticity diagram showing cone excitation by stimuli of equal
- luminance. Journal of the Optical Society of America, 69, 1183–1186. [PubMed] [CrossRef] [PubMed]
- Mareschal, I. Baker, Jr., C. L. (1998). Temporal and spatial response to second-order stimuli in cat area 18. Journal of Neurophysiology, 80, 2811–2823. [PubMed] [Article] [PubMed]
- McKeefry, D. J. Murray, I. J. Kulikowski, J. J. (2001). Red–green and blue–yellow mechanisms are matched in sensitivity for temporal and spatial modulation. Vision Research, 41, 245–255. [PubMed] [CrossRef] [PubMed]
- Medina, J. M. Mullen, K. T. (2009). Cross-orientation masking in human color vision. Journal of Vision, 9, (3):20, 1–16, <a href="http://journalofvision.org/9/3/20/">http://journalofvision.org/9/3/20/</a>, doi:<a href="http://journalofvision.org/9/3/20/">10.1167/9.3.20</a>. [Article] [CrossRef] [PubMed]
- Meese, T. S. Holmes, D. J. (2007). Spatial and temporal dependencies of cross-orientation suppression in human vision. Proceedings of the Royal Society B: Biological Sciences, 274, 127–136. [PubMed] [Article] [CrossRef]

Meier, L. Carandini, M. (2002). Masking by fast gratings. Journal of Vision, 2, (4):2, 293–301, <a href="http://journalofvision.org/2/4/2/">http://journalofvision.org/2/4/2/</a>, doi:10.1167/2.4.2. [PubMed] [Article] [CrossRef]

Metha, A. B. Mullen, K. T. (1996). Temporal mechanisms underlying flicker detection and identification for redgreen and achromatic stimuli. Journal of the Optical Society of America A, Optics, Image Science, and Vision, 13, 1969–1980. [PubMed] [CrossRef] [PubMed]

Metha, A. B. Mullen, K. T. (1997). Red–green and achromatic temporal filters: A ratio model predicts contrast-dependent speed perception. Journal of the Optical Society of America A, Optics, Image Science, and Vision, 14, 984–996. [PubMed] [CrossRef] [PubMed]

Mollon, J. D. (1989). "Tho' she kneel'd in that place where they grew..." The uses and origins of primate colour vision. Journal of Experimental Biology, 146, 21–38. [PubMed] [Article] [PubMed]

Morrone, M. C. Fiorentini, A. Burr, D. C. (1996). Development of the temporal properties of visual evoked potentials to luminance and colour contrast in infants. Vision Research, 36, 3141–3155. [PubMed] [PubMed]

Mullen, K. T. Boulton, J. C. (1992). Absence of smooth motion perception in color vision. Vision Research, 32, 483–488. [PubMed] [CrossRef] [PubMed]

Mullen, K. T. Cropper, S. J. Losada, M. A. (1997). Absence of linear subthreshold summation between red-green and luminance mechanisms over a wide range of spatio-temporal conditions. Vision Research, 37, 1157–1165. [PubMed] [CrossRef] [PubMed]

Muthukumaraswamy, S. D. Singh, K. D. (2008). Spatiotemporal frequency tuning of BOLD and gamma band MEG responses compared in primary visual cortex. Neuroimage, 40, 1552–1560. [PubMed] [CrossRef] [PubMed]

Norren, D. V. Padmos, P. (1974). Dark adaptation of separate cone systems studied with psychophysics and electroretinography. Vision Research, 14, 677–686. [PubMed] [CrossRef] [PubMed]

Priebe, N. J. Cassanello, C. R. Lisberger, S. G. (2003). The neural representation of speed in macaque area MT/V5. Journal of Neuroscience, 23, 5650–5661. [PubMed] [Article] [PubMed]

Rabin, J. Switkes, E. Crognale, M. Schneck, M. E. Adams, A. J. (1994). Visual evoked potentials in three-dimensional color space: Correlates of spatio-chromatic processing. Vision Research, 34, 2657–2671. [PubMed] [CrossRef] [PubMed]

Ramachandran, V. S. Gregory, R. L. (1978). Does colour provide an input to human motion perception? Nature, 275, 55–56. [PubMed] [CrossRef] [PubMed]

Robson, J. G. (1966). Spatial and temporal contrast sensitivity functions of the human visual system. Journal of the Optical Society of America A, 56, 1141–1142. [CrossRef]

Rushton, W. A. (1962). Visual pigments in man. Scientific American, 207, 120–132. [PubMed] [CrossRef] [PubMed]

Schiller, P. H. Finlay, B. L. Volman, S. F. (1976). Quantitative studies of single-cell properties in monkey striate

cortex II Orientation specificity and ocular dominance. Journal of Neurophysiology, 39, 1320–1333. [PubMed] [PubMed]

Schnapf, J. L. Kraft, T. W. Baylor, D. A. (1987). Spectral sensitivity of human cone photoreceptors. Nature, 325, 439–441. [PubMed] [CrossRef] [PubMed]

Shady, S. MacLeod, D. I. Fisher, H. S. (2004). Adaptation from invisible flicker. Proceedings of the National Academy of Sciences of the United States of America, 101, 5170–5173. [PubMed] [Article] [CrossRef] [PubMed]

Singh, K. D. Smith, A. T. Greenlee, M. W. (2000). Spatiotemporal frequency and direction sensitivities of human visual areas measured using fMRI. Neuroimage, 12, 550–564. [PubMed] [CrossRef] [PubMed]

Singh, M. Kim, S. Kim, T. S. (2003). Correlation between BOLD-fMRI and EEG signal changes in response to visual stimulus frequency in humans. Magnetic Resonance in Medicine, 49, 108–114. [PubMed] [CrossRef] [PubMed]

Snowden, R. J. Hess, R. F. (1992). Temporal frequency filters in the human peripheral visual field. Vision Research, 32, 61–72. [PubMed] [CrossRef] [PubMed]

Solomon, S. G. White, A. J. Martin, P. R. (1999). Temporal contrast sensitivity in the lateral geniculate nucleus of a New World monkey, the marmoset Callithrix jacchus. The Journal of Physiology, 517, 907–917. [PubMed] [Article] [CrossRef] [PubMed]

Sun, H. Smithson, H. E. Zaidi, Q. Lee, B. B. (2006). Specificity of cone inputs to macaque retinal ganglion cells. Journal of Neurophysiology, 95, 837–849. [PubMed] [Article] [CrossRef] [PubMed]

Sun, P. Ueno, K. Waggoner, R. A. Gardner, J. L. Tanaka, K. Cheng, K. (2007). A temporal frequency-dependent functional architecture in human V1 revealed by high-resolution fMRI. Nature Neuroscience, 10, 1404–1406. [PubMed] [CrossRef] [PubMed]

Swanson, W. H. Ueno, T. Smith, V. C. Pokorny, J. (1987). Temporal modulation sensitivity and pulse-detection thresholds for chromatic and luminance perturbations. Journal of the Optical Society of America A, Optics and Image Science, 4, 1992–2005. [PubMed] [CrossRef] [PubMed]

Switkes, E. Bradley, A. De Valois, K. K. (1988). Contrast dependence and mechanisms of masking interactions among chromatic and luminance gratings. Journal of the Optical Society of America A, Optics and Image Science, 5, 1149–1162. [PubMed] [CrossRef] [PubMed]

Ts'o, D. Y. Gilbert, C. D. (1988). The organization of chromatic and spatial interactions in the primate striate cortex. Journal of Neuroscience, 8, 1712–1727. [PubMed] [Article] [PubMed]

Uchikawa, K. Ikeda, M. (1986). Temporal integration of chromatic double pulses for detection of equal-luminance wavelength changes. Journal of the Optical Society of America A, Optics and Image Science, 3, 2109–2115. [PubMed] [CrossRef] [PubMed]

Vafaee, M. S. Meyer, E. Marrett, S. Paus, T. Evans, A. C. Gjedde, A. (1999). Frequency-dependent changes in cerebral metabolic rate of oxygen during activation of human visual cortex. Journal of Cerebral Blood Flow and Metabolism, 19, 272–277. [PubMed] [CrossRef] [PubMed]

Vimal, R. L. (1998). Color–luminance interaction: Data produced by oblique cross masking. Journal of the Optical Society of America A, Optics, Image Science, and Vision, 15, 1756–1766. [PubMed] [CrossRef] [PubMed]

Waugh, S. J. Hess, R. F. (1994). Suprathreshold temporal-frequency discrimination in the fovea and the periphery. Journal of the Optical Society of America A, Optics, Image Science, and Vision, 11, 1199–1212. [PubMed] [CrossRef] [PubMed]

Willis, A. Anderson, S. J. (2002). Colour and luminance interactions in the visual perception of motion. Proceedings of the Royal Society B: Biological Sciences, 269, 1011–1016. [PubMed] [Article] [CrossRef]

Yoshizawa, T. Mullen, K. T. Baker, Jr., C. L. (2003). Failure of signed chromatic apparent motion with luminance masking. Vision Research, 43, 751–759. [PubMed] [CrossRef] [PubMed]

Zheng, J. Zhang, B. Bi, H. Maruko, I. Watanabe, I. Nakatsuka, C. (2007). Development of temporal response properties and contrast sensitivity of V1 and V2 neurons in macaque monkeys. Journal of Neurophysiology, 97, 3905–3916. [PubMed] [Article] [CrossRef] [PubMed]

© 2009 ARVO